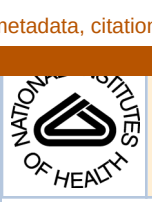

Published in final edited form as:
Mol Imaging. 2010 June ; 9(3): 117–127.

Advances in Molecular Imaging with Ultrasound

Ryan Gessner and **Paul A. Dayton**
Joint Department of Biomedical Engineering, University of North Carolina-North Carolina State University, Chapel Hill, NC

Abstract

Ultrasound imaging has long demonstrated utility in the study and measurement of anatomic features and noninvasive observation of blood flow. Within the last decade, advances in molecular biology and contrast agents have allowed researchers to use ultrasound to detect changes in the expression of molecular markers on the vascular endothelium and other intravascular targets. This new technology, referred to as ultrasonic molecular imaging, is still in its infancy. However, in preclinical studies, ultrasonic molecular imaging has shown promise in assessing angiogenesis, inflammation, and thrombus. In this review, we discuss recent advances in microbubble-type contrast agent development, ultrasound technology, and signal processing strategies that have the potential to substantially improve the capabilities and utility of ultrasonic molecular imaging.

Traditional non–contrast-enhanced ultrasound imaging uses a transducer to produce pulses of sound that propagate into tissue. These sound pulses are scattered from interfaces between tissue components of different density and compressibility. Scattered ultrasound reflections are detected and processed to form an image based on the intensity of scattered echoes and the time delay, which corresponds to the depth from which echoes have returned. As such, standard ultrasound imaging is well suited for assessment of anatomic features and measurement of blood flow in large vessels; however, there is no mechanism by which non–contrast-enhanced ultrasound can detect changes in physiology on a molecular level.

Contrast Agents

The fundamental enabling technology for ultrasonic molecular imaging is the contrast agent. Contrast agents for ultrasound imaging include microbubbles,[1–6] echogenic liposomes,[7–9] perfluorocarbon droplets,[10–12] and other materials such as gold particles,[13] which have a density and compressibility substantially different from that of blood and tissue. Highly compressible objects provide an additional advantage in that they can resonate in a sound field, producing a nonlinear acoustic response that enables detection strategies to segment the echoes from the contrast agent from those of tissue.[14–16] The supremely compressible gas core of microbubble contrast agents (MCAs) makes them uniquely echogenic, so even individual contrast agents can be detected with an ultrasound system.[17] It is for this reason that encapsulated microbubbles are the most prevalent form of contrast agent, and they are currently the only type of ultrasound contrast agent approved for clinical use in the United

Address reprint requests to: Paul A. Dayton, PhD, 304 Taylor Hall, 109 Mason Farm Road, Chapel Hill, NC 27599-6136; padayton@bme.unc.edu.

Financial disclosure of reviewers: None reported.

Financial disclosure of authors: This Dayton lab is supported by the National Institutes of Health through R01 EB009066, R01 EB008733, and the NIH Roadmap for Medical Research through R21EB005325. Intramural support is provided from the University of North Carolina Lineberger Cancer Center. P. A. Dayton has ongoing research with Siemens Medical Systems, Visualsonics, and Lantheus Medical Imaging, none of which involves financial sponsorship, and is a member of the Scientific Advisory Board for Targeson, LLC.

States and Europe. Owing to the widespread research on and implementation of MCAs, the technology discussed in this review pertains primarily to this type of contrast agent.

MCAs typically consist of a high-molecular-weight gas core stabilized with a lipid, protein, sugar, or polymer.[18,19] Early-generation MCAs contained nitrogen or air; however, perfluorocarbons and sulfur hexafluoride are now preferred owing to their low solubility in blood and poor diffusivity through the encapsulating shell, which extends microbubble circulation time in vivo.[19,20]

Although nontargeted contrast agents are used clinically for assessing blood perfusion, particularly in cardiology, molecularly targeted agents have still not received clinical approval. Molecularly targeted contrast agents have a formulation similar to that of nontargeted agents, except that they incorporate an adhesion mechanism in their shell so that they can bind to cells expressing molecular signatures of pathology in vivo. Commonly used adhesion ligands include peptides,[21,22] antibodies,[23,24] and disintegrins[25,26] but may also include peptidomimetics or other adhesion ligands that can be conjugated directly to the contrast agent shell.[27,28]

Ultrasound Molecular Imaging

Molecular imaging is commonly associated with modalities such as positron emission tomography (PET), single-photon emission computed tomography (SPECT), and optical imaging; ultrasound, however, has several advantages over these and other imaging modalities. Ultrasound systems are low cost, portable (and becoming even more so with shrinking electronic components), and safe for both the user and the patient over repeated use because of the lack of ionizing radiation. Additionally, ultrasound is a high frame rate, real-time imaging modality, and has a better depth of penetration than optical imaging. Finally, ultrasound has the unique ability to disrupt (clear) contrast agents,[29,30] to manipulate their distribution through radiation force,[31] and to combine therapy with imaging, allowing true implementation of “theranostics.”[27,32–35]

Molecular imaging with ultrasound is typically performed as follows: an ultrasound transducer is fixed in position over the region of interest with a mechanical arm to avoid motion artifacts from operator movement. A targeted contrast agent is administered into the peripheral vasculature, often through a tail vein during serial imaging studies in rodents. Prior to imaging, a waiting period of approximately 4 to 30 minutes is required, depending on contrast agent circulation characteristics.[36] During this period, there is a first phase when the targeted contrast agents accumulate in the microvasculature, followed by a second phase when freely circulating agents are cleared from the animal’s system. After free agent clearance, imaging is performed to detect molecularly targeted contrast agents retained in regions of pathologic tissue. When possible, a first acquisition of several imaging frames is followed by a destruction pulse, which clears all contrast within the field of view. A second set of imaging frames can then be gathered as a no-contrast baseline to quantify image intensity increase owing to molecularly targeted agents.

Challenges in Molecular Imaging with Ultrasound

Although ultrasonic molecular imaging has made significant progress over the last decade, this technology still faces several challenges before it can rise to its full diagnostic potential. It is the ideal goal of this technology to determine if a molecular target is present and, if so, to what degree. This requires that the contrast agents specifically adhere to their molecular target and bind in quantities great enough to overwhelm the signal contributions from nonspecific retention. Additionally, the ultrasound system should have sufficient sensitivity to detect the targeted agents present at the site of pathology and be able to assess the

pathology in its entirety. In this review, we hypothesize that several limitations have slowed the progression of ultrasonic molecular imaging; however, recent advances in contrast agent development, ultrasound technology, and detection strategies demonstrate the potential to substantially improve the capabilities and utility of ultrasonic molecular imaging. We review these challenges and recent advances in the following sections.

Low Numbers of Retained Contrast Agents

Given that the magnitude of the detected ultrasound signal is a function of the quantity of contrast agents retained at the site of target endothelium, it is intuitive that the retention of targeted contrast agents at a site of diseased tissue should be maximized, whereas nonspecific contrast retention should also be minimized. For molecular imaging studies in small animals, the injected concentration of microbubbles is typically on the order of 10^7 to 10^8 bubbles/kg. Prior studies assessing the adhesion of targeted microbubbles have observed only small amounts of targeted contrast retained in vivo, on the order of several bubbles per cubic millimeter.[25,37] Correspondingly, video intensity from targeted agents in vivo is typically only several fold higher than background.[23,26,38,39]

High Background from Freely Circulating Agents

The high background signal from freely circulating contrast agents further complicates the ability to detect small numbers of adherent targeted contrast agents. With the large total injected dose of contrast and the very small percentage of the total dose that is retained in target microvasculature, the scattered ultrasound signal from nontargeted contrast overwhelms signal from targeted contrast.[40–42] As previously mentioned, the current technique for molecular imaging deals with this limitation through a waiting period (Figure 1). After injection of the bolus of targeted contrast agent, a waiting period between several and tens of minutes is implemented prior to imaging. During this time, freely circulating microbubbles are slowly cleared from the circulation by the reticuloen-dothelial system, nonspecific retention, and bubble deterioration.[43–45] Although this waiting technique is not a significant challenge in a molecular imaging procedure, it is possible that a percentage of microbubbles retained at the target site both detach and degrade over this time period, reducing the method's sensitivity.

Limited Field of View

One limitation of ultrasound imaging, in general, compared to modalities such as computed tomography (CT), magnetic resonance imaging (MRI), PET, and SPECT, is a smaller field of view. Until fairly recently, ultrasound imaging was largely a two-dimensional modality, depicting only a single image slice through tissue. In diagnostic imaging, the real-time imaging capability compensates for this as it allows a sonographer to scan through the tissue of interest to view or measure target features. In ultrasonic molecular imaging, however, most current protocols involve maintaining the transducer fixed in a clamp to observe the same slice of tissue. This is usually required because quantifiable measurement of signal from contrast involves a background subtraction after a destructive pulse, which creates artifacts in the presence of tissue or transducer motion. Recent advances in transducer technology have led to the implementation of matrix array transducers, allowing real-time three-dimensional ultrasound imaging (also called four-dimensional, considering the time dimension). Three-dimensional ultrasound is still relatively new to the clinic and is used primarily in obstetrics and cardiology. However, due to the complicated pulse sequences required to differentiate MCAs from surrounding tissue, three-dimensional contrast imaging has been challenging to implement on matrix array probes. Although some ultrasound system manufacturers currently have real-time three-dimensional contrast imaging capability, the performance of contrast imaging modes on matrix array transducers still falls short of the resolution and contrast detection capability available on transducers for two-

dimensional imaging. Hence, to date, ultrasonic molecular imaging has been largely limited to a single slice of tissue.

Quantitative Ability

An ideal goal of any imaging modality is to achieve a quantitative measurement. Although non–contrast-enhanced ultrasound can reliably allow anatomic measurements, contrast-enhanced ultrasound imaging is still largely qualitative and based on relative video intensity changes. The precise relationship between the number and distribution of retained targeted MCAs in tissue and the resulting acoustic response is still unknown. The scattered signal from a targeted MCA is a complex function of the microbubble size,[46,47] the damping effects of the surroundings,[48–50] and interactions with other local MCAs.[51] Additionally, the ultrasound response is attenuated by tissue, both as a function of depth and as a function of tissue type. Until an imaging system is able to estimate the number of microbubbles retained in tissue, it will be challenging to perform accurate quantitative measurements of molecular marker expression with ultrasonic imaging.

Possible Immune Responses

For contrast agents used in ultrasound molecular imaging studies, there is the possibility of an immunogenic response triggered by contrast agent components or the various targeting ligand compositions on their surfaces. To date, clinical studies have not been reported with molecularly targeted contrast agents, and preclinical and clinical imaging studies using nontargeted microbubbles have been associated with hypersensitivity reactions only in rare cases.[52–54] However, in preclinical studies, researchers have observed enhanced complement activation, reduced circulation time, and nonspecific adhesion associated with MCAs as a function of their shell components.[42,55,56]

Advances in Molecular Imaging with Ultrasound

Although the aforementioned challenges provide some limitations to molecular imaging with ultrasound, recent advances in technology have demonstrated that many of these limitations can be ameliorated. In the next sections, we review several technologies and approaches that are notable improvements in ultrasonic molecular imaging.

Contrast Agents

New and Multiligand Approaches—To improve contrast agent retention at the desired target site, many groups are pursuing mechanisms to improve agent-endothelium adhesion with new approaches. Several groups have demonstrated enhanced microbubbles targeting through the use of multiple adhesion ligands (Figure 2A).[57–59] To improve targeting of microbubbles to inflamed tissues, both Weller and colleagues and Ferrante and colleagues have modeled their targeted contrast agents after biologic leukocytes by incorporating ligands targeted to both selectins and immunoglobulin adhesion molecules.[57,58] Proinflammatory selectins (such as E and P selectin) are naturally expressed by surface endothelial cells, thus promoting the rolling action of leukocytes. Immunoglobulin adhesion molecules (such as intercellular adhesion molecule 1 [ICAM-1] and vascular cell adhesion molecule 1 [VCAM-1]) promote the firm binding of leukocytes and the transmigration of leukocytes into tissue in regions where these proteins are expressed. The incorporation of both types of binding mechanisms in microbubble shells resulted in a significantly improved targeting efficiencies of between 50 and 300% when compared to bubbles bearing only a single targeting ligand.[58] The mechanism for this improvement is hypothesized to be due to the rolling action of contrast agents along the blood vessel wall facilitated by selectin adhesion, which improves the likelihood of a longer-lasting integrin bond forming at the target site.

Another method to improve the likelihood of micro-bubble targeting has been demonstrated by altering ligand architecture. Klibanov and colleagues demonstrated that polymeric forms of sialyl Lewis^x (Figure 2B) were more efficient at binding to models of inflammation both in vitro and in vivo than antibody-mediated targeting.60 Although the two demonstrated comparable targeting efficiencies at a slow flow rate (0.68 dyne/cm^2 shear stress), the efficiency of the antibody-mediated targeted contrast agents was reduced by more than 20-fold at a fast flow rate (4.45 dyne/cm^2 shear stress).60

Bubble Size Optimization—Size is one of the most important parameters in micro-bubble acoustic response. Microbubble diameter is directly related to scattering cross section,61 resonant frequency,62 destruction threshold,63 nonlinear oscillation,64 and susceptibility to radiation force.65 Additionally, in the size range typically used for contrast imaging (≈1–7 μm), the changes in resonant frequency as a function of diameter are substantial.66 This means that for a polydisperse contrast agent population, it is unlikely that all of the contrast agents will be in the diameter range optimized for imaging, radiation force–mediated displacement, or clearance (destruction). Most MCAs are produced with technologies that result in a size distribution with a large variance. With traditional contrast-enhanced ultrasound imaging, there has been little need to consider contrast agent size distribution. This is largely due to the fact that millions to billions of microbubbles can be injected into a patient during an imaging examination.67 However, in molecular imaging, where low contrast retention is already an issue, it is important to be maximally sensitive to the entire contrast agent population. Talu and colleagues demonstrated that contrast agents with a uniform size distribution produce a substantially more correlated acoustic response than polydisperse populations and that a monodisperse population of MCAs can be more easily tailored to match the imaging system's frequency for optimal acoustic response.68 It is hypothesized that microbubble monodispersity will likely be required to elucidate quantifiable information from molecular imaging studies.69

Given that the diameter of microbubbles plays a direct role in echogenicity, several researchers have examined the potential of improving ultrasound contrast sensitivity by altering microbubble size distribution. In vitro studies of monodisperse microbubbles by Kaya and colleagues demonstrated that a severalfold increase in echogencity could be achieved by increasing microbubble diameter (Figure 3).47 Sirsi and colleagues used high-frequency (40 MHz) imaging for studying perfusion in the mouse kidney and observed that contrast intensity doubled for microbubbles of 4 to 5 μm in mean diameter compared to bubbles with a 1 to 2 μm mean diameter.70 Contrast enhancement was improved even more with 6 to 8 μm MCAs. The advantages of size-sorted MCAs in molecular imaging applications were demonstrated by Streeter and colleagues in a rat tumor model using nonlinear imaging at 8 MHz, where sorted 3 μm MCAs were observed to provide a 20-fold improvement in sensitivity over polydisperse 1 μm MCAs (Figure 4).36 Neither Sirsi and colleagues nor Streeter and colleagues observed limitations in microbubble circulation owing to the size of the larger microbubbles; in contrast, signals from larger microbubbles were observed to persist for a period of time several times greater than smaller microbubbles. Although these results suggest that larger bubbles are better suited for molecular imaging with ultrasound, additional studies to examine the trade-off between adhesion efficiency versus signal intensity as a function of microbubble size have yet to be performed.

Creating bubbles of uniform sizes and varying mean diameters can be achieved with technology such as microfluidics,71–74 electrohydrodynamic atomization,75 differential centrifugation,76 and other formulation techniques.69,77 Although these new formulation techniques have been successful in providing monodisperse or size-selected microbubbles in small amounts, in general, their complexity and low production rate are still limiting factors

in the ability to produce sufficient size-optimized bubbles in commercially available quantity.

Bubble and Shell Architecture—Modeling targeted microbubbles after their naturally occurring analogues, leukocytes, is an intuitive strategy for optimizing their targeting efficiency. One of the distinct differences between these two targeting agents—bubbles and leukocytes—is their structural morphology during targeting events. Leukocytes are known to become more deformable on chemical activation as a result of cytoskeletal rearrangements. This increased deformability increases their contact area with the endothelial surface, which also simultaneously increases the number of potential bonds with the endothelium and decreases the load per bond formed. It has been hypothesized that the relative structural rigidity of bubbles compared to leukocytes is partially responsible for their poor retention rates at their desired target sites as fewer bonds formed implies higher stresses applied to each of them after targeting and thus a greater likelihood of detachment.78 Rychak and colleagues demonstrated the means to create bubbles with excess deformable lipid in their shells (Figure 2C), resulting in a greater deformability.78 These deformable, or "wrinkly," bubbles were more effective in molecular imaging studies targeted to the inflammatory protein P-selectin, both in vitro and in vivo, at forming stable bonds at their target sites. Relative to spherical bubbles, bubbles with excess surface lipid showed significantly better sustained targeting efficiency in vitro at wall shear stresses between 0.34 and 1.3 dyne/cm^2, as well as at targeting site densities between 7 and 109 sites/μm^2. The in vivo retention rate of wrinkly bubbles was twice that of spherical bubbles, as determined by intravital microscopy in a cremaster muscle of a mouse model of inflammation (Figure 5).

Reduction in Immunogenicity—It has been possible to significantly reduce complement activation from targeted microbubbles by implementing buried-ligand architectures (Figure 2D).55,56 With this technique, both the polyethylene glycol brush chains and targeting ligand chains are conjugated to the lipid shell of the contrast agents. The brush chains are longer than the ligand chains and thus veil the ligands from the various blood components that could otherwise trigger an immunogenic reaction. Borden and colleagues demonstrated that buried-ligand architectures were able to help isolate the targeting ligands from their surroundings until the bubbles were intentionally activated with an acoustic radiation force pulse, which transiently revealed the buried ligand to the target site.55 The strategy showed a significant improvement over conventional exposed-ligand micro-bubbles in avoiding immunogenic responses (Figure 6).

Imaging and Detection Technology

Real-Time Molecular Imaging—To overcome the challenge of detecting small numbers of retained targeted contrast agents with a high background of freely circulating agents without a waiting period, several groups have been developing real-time molecular imaging approaches. Zhao and colleagues proposed two methods to help accomplish this goal of real-time imaging of bound contrast agents.40 The first "image-push-image" method improves imaging sensitivity by increasing the number of adherent agents via a radiation force push of contrast agents toward the distal wall of the blood vessel. The prepush image is subtracted from the postpush image to yield the signal from adherent agents. The second real-time ultrasound molecular imaging strategy proposed in that article was to implement a "slow-time" filtering approach in which successive frames are low-pass filtered such that rapidly changing signals (namely those from nonstationary bubbles) are removed from the image data (Figure 7). Because both adherent bubbles and tissue are equivalently stationary, this second strategy necessitates a contrast-specific imaging technique with a high degree of tissue suppression. Real-time molecular imaging methods have been demonstrated in vitro with several different contrast-specific methods, including subharmonic imaging79 and

pulse inversion.80 Zheng and colleagues and Gessner and colleagues recently demonstrated application of dual-frequency transducers and pulse sequences designed for production of radiation force and real-time targeted MCA detection without a waiting period.81,82

Low Mechanical Index Imaging—MCAs are destroyed by ultrasound energy, primarily as a function of microbubble diameter, acoustic frequency, and acoustic amplitude.63 Low–mechanical index imaging strategies use low amplitudes and higher frequencies to minimize MCA destruction. These imaging strategies are advantageous because of their ability to image adherent targeted contrast agents over time after a single administration. Additionally, nondestructive imaging will likely be required to facilitate three-dimensional and quantitative molecular imaging as destructive imaging techniques require that all of the signal from targeted contrast agents must be acquired during the first imaging pulse to which the contrast agents are exposed, which is practically challenging.

Many commercial imaging systems now include low–mechanical index contrast imaging modes, such as (but not limited to) Cadence contrast pulse sequence (CPS, Siemens, Mountain View, CA)26,83 and contrast harmonic imaging (CHI, Philips, Bothell, WA).84,85 Recently, Needles and colleagues demonstrated the application of low–mechanical index contrast imaging modes at frequencies greater than 15 MHz on a high-frequency array system.86

Volumetric Imaging—Recent studies by Gessner and colleagues82 and Streeter and colleagues (Figure 8; unpublished data, 2009) demonstrated the utility of three-dimensional molecular imaging. By acquiring multiple two-dimensional images via a motorized stage and reconstructing the data offline, heterogeneities within pathologic tissue volumes are observed that would be impossible to assess with traditional single-slice molecular imaging. Three-dimensional contrast imaging capabilities are currently in development,85,87 and continued improvements in low–mechanical index, high–resolution, three-dimensional imaging will soon allow for the full volumetric characterization of tissue pathologies. This will ensure consistent data collection in longitudinal studies by avoiding the possibility of undersampling heterogeneous tissues.

Improvements in Microbubble Delivery

Radiation Force–Enhanced Targeting—For highly compressible objects such as MCAs, acoustic radiation force can be of a substantial magnitude even at low acoustic pressures.65 A transducer directing energy perpendicular to flow in a vessel can displace moving MCAs to the wall of the vessel opposite the sound source and greatly enhance microbubble–endothelium interactions. Dayton and colleagues previously proposed this mechanism for enhanced targeting of microbubbles because radiation force both decreases ligand-receptor distances and reduces the flow velocity of microbubbles in a vessel.88 The capability of radiation force to enhance targeted MCA retention was observed in vivo with intravital microscopy by Rychak and colleagues89 and acoustically by Gessner and colleagues.82 In a rat model of angiogenesis, application of radiation force prior to imaging demonstrated a sevenfold increase in image intensity compared to the control case (Figure 9).82 This application of radiation force to enhance retention of targeted microbubbles is particularly attractive for applications that use microbubbles as therapeutic vehicles.

Submicron Contrast Agents—A significant limitation of traditional MCAs is that their several-micron diameter range retains these agents to the vascular space. Several attempts have been made to overcome this limitation. Submicron (< 1 μm) microbubbles have been formulated with polymer shells. Although the extravasation potential of these agents has not been confirmed, Patel and colleagues demonstrated their acoustic activity,90,91 and Wisner

and colleagues used these sub-micron agents for lymphographic ultrasound imaging.92 Gao demonstrated that stabilized liquid perfluorocarbon nanodroplets can be formulated with a diameter range small enough to extravasate but then can be vaporized into microgas bubbles by a combination of body temperature and ultrasound energy.93 Once vaporized, these vehicles are detectable with ultrasound similar to MCAs. Thus, it is likely that contrast agents can be prepared to exit the vascular space, particularly in regions of leaky tumor vasculature, which is not currently possible with MCAs.

Conclusion

Molecular imaging with ultrasound is an exciting field because it adds a new dimension of diagnostic capability to this already ubiquitous modality. It is certain that the future role of ultrasound in medicine will continue to increase owing to its safety and convenience. Already some manufacturers are producing diagnostic systems no larger than a cellular phone that are intended to be as widely available as stethoscopes. With advancing understanding in molecular changes involved in disease progression, molecular imaging will enable detection of pathology and observation of response to treatment before phenotypic changes occur.

As illustrated in this review, technology already exists to increase the sensitivity of ultrasound to contrast agents severalfold through tailoring contrast agent size distribution. Improving the monodispersity of the contrast agent population will remove a substantial variable limiting the ability to perform quantifiable contrast measurements. Modifying shell structure and ligand architecture can provide targeted contrast agents with better retention characteristics and reduced immunogenicity. Transducers and signal processing are being developed to detect targeted contrast agents nondestructively, with high contrast to tissue ratios, and in real time despite background signal from freely circulating contrast. The application of radiation force has been shown to increase the amount of targeted contrast agents retained at a target site in vivo, which is important not only for molecular imaging but also for targeted drug delivery through acoustically active carrier vehicles. Finally, the development of phase change and submicron contrast agents will enable ultrasound contrast to reach beyond the limits of the endothelium.

Acknowledgments

We appreciate the assistance of Dr. Joshua Rychak in editing the scientific content and the assistance of Steven Feingold, Jason Streeter, and Paul Kogan in preparing figures and references.

References

1. Keller MW, Glasheen W, Kaul S. Albunex: a safe and effective commercially produced agent for myocardial contrast echocardiography. J Am Soc Echocardiogr. 1989; 2:48–52. [PubMed: 2627424]
2. Smith MD, Elion JL, McClure RR, et al. Left heart opacification with peripheral venous injection of a new saccharide echo contrast agent in dogs. J Am Coll Cardiol. 1989; 13:1622–8. [PubMed: 2723275]
3. Klibanov, AL. Ultrasound contrast agents: development of the field and current status. In: Krause, W., editor. Contrast agents II. Vol. 222. New York: Springer-Verlag; 2002. p. 73-106.
4. Stride E. Physical principles of microbubbles for ultrasound imaging and therapy. Cerebrovasc Dis. 2009; 27 (Suppl 2):1–13. [PubMed: 19372656]
5. Dayton PA, Ferrara KW. Targeted imaging using ultrasound. J Magn Reson Imaging. 2002; 16:362–77. [PubMed: 12353252]
6. de Jong N, Bouakaz A, Frinking P. Basic acoustic properties of microbubbles. Echocardiography. 2002; 19:229–40. [PubMed: 12022933]

7. Alkan-Onyuksel H, Demos SM, Lanza GM, et al. Development of inherently echogenic liposomes as an ultrasonic contrast agent. J Pharm Sci. 1996; 85:486–90. [PubMed: 8742939]
8. Tiukinhoy-Laing SD, Buchanan K, Parikh D, et al. Fibrin targeting of tissue plasminogen activator-loaded echogenic liposomes. J Drug Target. 2007; 15:109–14. [PubMed: 17365281]
9. Klegerman ME, Zou Y, McPherson DD. Fibrin targeting of echogenic liposomes with inactivated tissue plasminogen activator. J Liposome Res. 2008; 18:95–112. [PubMed: 18569446]
10. Mattrey RF. The potential role of perfluorochemicals (PFCs) in diagnostic-imaging. Artific Cells Blood Substit Immobil Biotechnol. 1994; 22:295–313.
11. Marsh JN, Partlow KC, Abendschein DR, et al. Molecular imaging with targeted perfluorocarbon nanoparticles: quantification of the concentration dependence of contrast enhancement for binding to sparse cellular epitopes. Ultrasound Med Biol. 2007; 33:950–8. [PubMed: 17434667]
12. Wickline SA, Hughes M, Ngo FC, et al. Blood contrast enhancement with a novel, non-gaseous nanoparticle contrast agent. Acad Radiol. 2002; 9 (Suppl 2):S290–3. [PubMed: 12188251]
13. Korosoglou G, Behrens S, Bekeredjian R, et al. The potential of a new stable ultrasound contrast agent for site-specific targeting. An in vitro experiment. Ultrasound Med Biol. 2006; 32:1473–8. [PubMed: 17045866]
14. Burns PN, Hope Simpson D, Averkiou MA. Nonlinear imaging. Ultrasound Med Biol. 2000; 26 (Suppl 1):S19–22. [PubMed: 10794866]
15. Forsberg F, Shi WT, Goldberg BB. Subharmonic imaging of contrast agents. Ultrasonics. 2000; 38(1–8):93–8. [PubMed: 10829636]
16. Frinking PJ, Bouakaz A, Kirkhorn J, et al. Ultrasound contrast imaging: current and new potential methods. Ultrasound Med Biol. 2000; 26:965–75. [PubMed: 10996696]
17. Klibanov AL, Rasche PT, Hughes MS, et al. Detection of individual microbubbles of ultrasound contrast agents—imaging of free-floating and targeted bubbles. Invest Radiol. 2004; 39:187–95. [PubMed: 15076011]
18. Goldberg, BB.; Raichlen, JS.; Forsberg, F. Ultrasound contrast agents: basic principles and clinical applications. London: Martin Dunitz; 2001.
19. Borden, MA.; Dayton, PA. Targeted ultrasound contrast agents. In: Pomper, MG.; Gelovani, JG., editors. Molecular imaging in oncology. New York: Informa Healthcare USA; 2009. p. 329-43.
20. Cohen JL, Cheirif J, Segar DS, et al. Improved left ventricular endocardial border delineation and opacification with OPTISON (FS069), a new echocardiographic contrast agent. Results of a phase III multicenter trial. J Am Coll Cardiol. 1998; 32:746–52. [PubMed: 9741522]
21. Unger EC, McCreery TP, Sweitzer RH, et al. In vitro studies of a new thrombus-specific ultrasound contrast agent. Am J Cardiol. 1998; 81(12A):58G–61G.
22. Tweedle MF. Peptide-targeted diagnostics and radiotherapeutics. Acc Chem Res. 2009; 42:958–68. [PubMed: 19552403]
23. Kaufmann BA, Carr CL, Belcik JT, et al. Molecular imaging of the initial inflammatory response in atherosclerosis: implications for early detection of disease. Arterioscler Thromb Vasc Biol. 2010; 30(1):54–9. [PubMed: 19834105]
24. Weller GE, Lu E, Csikari MM, et al. Ultrasound imaging of acute cardiac transplant rejection with microbubbles targeted to intercellular adhesion molecule-1. Circulation. 2003; 108:218–24. [PubMed: 12835214]
25. Leong-Poi H, Christiansen J, Klibanov AL, et al. Noninvasive assessment of angiogenesis by ultrasound and microbubbles targeted to alpha(v)-integrins. Circulation. 2003; 107:455–60. [PubMed: 12551871]
26. Stieger SM, Dayton PA, Borden MA, et al. Imaging of angiogenesis using Cadence contrast pulse sequencing and targeted contrast agents. Contrast Media Mol Imaging. 2008; 3:9–18. [PubMed: 18335479]
27. Lanza GM, Wickline SA. Targeted ultrasonic contrast agents for molecular imaging and therapy. Curr Probl Cardiol. 2003; 28:625–53. [PubMed: 14691443]
28. Villanueva FS. Molecular imaging of cardiovascular disease using ultrasound. J Nucl Cardiol. 2008; 15:576–86. [PubMed: 18674725]

29. Walker KW, Pantely GA, Sahn DJ. Ultrasound-mediated destruction of contrast agents. Effect of ultrasound intensity, exposure, and frequency. Invest Radiol. 1997; 32:728–34. [PubMed: 9406012]
30. Chomas JE, Dayton P, Allen J, et al. Mechanisms of contrast agent destruction. IEEE Trans Ultrason Ferroelectr Freq Control. 2001; 48:232–48. [PubMed: 11367791]
31. Dayton PA, Morgan KE, Klibanov ALS, et al. A preliminary evaluation of the effects of primary and secondary radiation forces on acoustic contrast agents. IEEE Trans Ultrason Ferroelectr Freq Control. 1997; 44:1264–77.
32. Ferrara KW, Borden MA, Zhang H. Lipid-shelled vehicles: engineering for ultrasound molecular imaging and drug delivery. Acc Chem Res. 2009; 42:881–92. [PubMed: 19552457]
33. Ferrara KW, Pollard RE, Borden MA. Ultrasound microbubble contrast agents: fundamentals and application to drug and gene delivery. Annu Rev Biomed Eng. 2007; 9:415–47. [PubMed: 17651012]
34. Bohmer MR, Klibanov AL, Tiemann K, et al. Ultrasound triggered image-guided drug delivery. Eur J Radiol. 2009; 70:242–53. [PubMed: 19272727]
35. Hernot S, Klibanov AL. Microbubbles in ultrasound-triggered drug and gene delivery. Adv Drug Deliv Rev. 2008; 60:1153–66. [PubMed: 18486268]
36. Streeter JE, Gessner R, Miles I, et al. Improving sensitivity in ultrasound molecular imaging by tailoring contrast agent size distribution: in vivo studies. Mol Imaging. [In press]. 10.2310/7290.2010.00005
37. Schumann PA, Christiansen JP, Quigley RM, et al. Targeted-microbubble binding selectively to GPIIb IIIa receptors of platelet thrombi. Invest Radiol. 2002; 37:587–93. [PubMed: 12393970]
38. Lindner JR, Song J, Christiansen J, et al. Ultrasound assessment of inflammation and renal tissue injury with microbubbles targeted to P-selectin. Circulation. 2001; 104:2107–12. [PubMed: 11673354]
39. Weller GER, Wong MKK, Modzelewski RA, et al. Ultrasonic imaging of tumor angiogenesis using contrast microbubbles targeted via the tumor-binding peptide arginine-arginine-leucine. Cancer Res. 2005; 65:533–9. [PubMed: 15695396]
40. Zhao S, Kruse DE, Ferrara KW, et al. Selective imaging of adherent targeted ultrasound contrast agents. Phys Med Biol. 2007; 52:2055–72. [PubMed: 17404455]
41. Christiansen JP, Lindner JR. Molecular and cellular imaging with targeted contrast ultrasound. Proc IEEE Ultrason Symp. 2005; 93:809–18.
42. Lindner JR. Contrast ultrasound molecular imaging of inflammation in cardiovascular disease. Cardiovasc Res. 2009; 84:182–9. [PubMed: 19783842]
43. Walday P, Tolleshaug H, Gjoen T, et al. Biodistributions of air-filled albumin microspheres in rats and pigs. Biochem J. 1994; 299(Pt 2):437–43. [PubMed: 8172604]
44. Fisher NG, Christiansen JP, Klibanov A, et al. Influence of microbubble surface charge on capillary transit and myocardial contrast enhancement. J Am Coll Cardiol. 2002; 40:811–9. [PubMed: 12204515]
45. Willmann JK, Cheng Z, Davis C, et al. Targeted microbubbles for imaging tumor angiogenesis: assessment of whole-body biodistribution with dynamic micro-PET in mice. Radiology. 2008; 249:212–9. [PubMed: 18695212]
46. Sijl J, Gaud E, Frinking PJ, et al. Acoustic characterization of single ultrasound contrast agent microbubbles. J Acoust Soc Am. 2008; 124:4091–7. [PubMed: 19206831]
47. Kaya M, Feingold S, Streeter JE, et al. Acoustic characterization of individual monodisperse contrast agents with an optical-acoustical system. Proc IEEE Ultrasonics Symp. 2009:1813–1816.
48. Caskey CF, Kruse DE, Dayton PA, et al. Microbubble oscillation in tubes with diameters of 12, 25, and 195 microns. Appl Phys Lett. 2006; 88:033902.
49. Dollet B, van der Meer SM, Garbin V, et al. Nonspherical oscillations of ultrasound contrast agent microbubbles. Ultrasound Med Biol. 2008; 34:1465–73. [PubMed: 18450362]
50. Zhao S, Ferrara KW, Dayton PA. Asymmetric oscillation of adherent targeted ultrasound contrast agents. Appl Phys Lett. 2005; 87:nihms8459. [PubMed: 16755307]

51. Allen JS, Kruse DE, Dayton PA, et al. Effect of coupled oscillations on microbubble behavior. J Acoust Soc Am. 2003; 114:1678–90. [PubMed: 14514221]
52. Geleijnse ML, Nemes A, Vletter WB, et al. Adverse reactions after the use of sulphur hexafluoride (SonoVue) echo contrast agent. J Cardiovasc Med (Hagerstown). 2009; 10:75–7. [PubMed: 19145117]
53. Asch FM, Weissman NJ. Overview of the 2008 Food and Drug Administration Advisory Committee on safety considerations in the development of ultrasound contrast agents. Circulation. 2009; 119:1956–61. [PubMed: 19364988]
54. Yamaya Y, Niizeki K, Kim J, et al. Anaphylactoid response to Optison(R) and its effects on pulmonary function in two dogs. J Vet Med Sci. 2004; 66:1429–32. [PubMed: 15585961]
55. Borden MA, Sarantos MR, Stieger SM, et al. Ultrasound radiation force modulates ligand availability on targeted contrast agents. Mol Imaging. 2006; 5:139–47. [PubMed: 16954028]
56. Borden MA, Zhang H, Gillies RJ, et al. A stimulus-responsive contrast agent for ultrasound molecular imaging. Biomaterials. 2008; 29:597–606. [PubMed: 17977595]
57. Weller GER, Villanueva FS, Tom EM, et al. Targeted ultrasound contrast agents: in vitro assessment of endothelial dysfunction and multi-targeting to ICAM-1 and sialyl Lewis. Biotechnol Bioeng. 2005; 92:780–8. [PubMed: 16121392]
58. Ferrante EA, Pickard JE, Rychak J, et al. Dual targeting improves microbubble contrast agent adhesion to VCAM-1 and P-selectin under flow. J Control Release. 2009; 140:100–7. [PubMed: 19666063]
59. Willmann JK, Lutz AM, Paulmurugan R, et al. Dual-targeted contrast agent for US assessment of tumor angiogenesis in vivo. Radiology. 2008; 248:936–44. [PubMed: 18710985]
60. Klibanov AL, Rychak JJ, Yang WC, et al. Targeted ultrasound contrast agent for molecular imaging of inflammation in high-shear flow. Contrast Media Mol Imaging. 2006; 1:259–66. [PubMed: 17191766]
61. Quaia, E. Contrast media in ultrasonography: basic principles and clinical applications. Berlin: Springer-Verlag; 2005.
62. Doinikov AA, Haac JF, Dayton PA. Resonance frequencies of lipid-shelled microbubbles in the regime of nonlinear oscillations. Ultrasonics. 2009; 49:263–8. [PubMed: 18977009]
63. Chomas JE, Dayton P, May D, et al. Threshold of fragmentation for ultrasonic contrast agents. J Biomed Optics. 2001; 6:141–50.
64. de Jong N, Emmer M, Chin CT, et al. “Compression-only” behavior of phospholipid-coated contrast bubbles. Ultrasound Med Biol. 2007; 33:653–6. [PubMed: 17320268]
65. Dayton PA, Allen JS, Ferrara KW. The magnitude of radiation force on ultrasound contrast agents. J Acoust Soc Am. 2002; 112(5 Pt 1):2183–92. [PubMed: 12430830]
66. Khismatullin DB. Resonance frequency of microbubbles: effect of viscosity. J Acoust Soc Am. 2004; 116:1463–73. [PubMed: 15478411]
67. Definity North Billerica, MA: Lantheus Medical Imaging; 2008.
68. Talu E, Hettiarachchi K, Zhao S, et al. Tailoring the size distribution of ultrasound contrast agents: possible method for improving sensitivity in molecular imaging. Mol Imaging. 2007; 6:384–92. [PubMed: 18053409]
69. Stride E, Tang MX, Eckersley RJ. Physical phenomena affecting quantitative imaging of ultrasound contrast agents. Appl Acoust. 2009; 70:1352–62.
70. Sirsi S, Feshitan J, Homma S, et al. High-frequency ultrasound imaging of size isolated microbubbles in mice. Proc IEEE Ultrason Symp. 2009:271–274.
71. Garstecki P, Gitlin I, DiLuzio W, et al. Formation of monodisperse bubbles in a microfluidic flow-focusing device. Appl Phys Lett. 2004; 85:2649–51.
72. Hettiarachchi K, Talu E, Longo ML, et al. On-chip generation of microbubbles as a practical technology for manufacturing contrast agents for ultrasonic imaging. Lab Chip. 2007; 7:463–8. [PubMed: 17389962]
73. Talu E, Hettiarachchi K, Powell RL, et al. Maintaining mono-dispersity in a microbubble population formed by flow-focusing. Langmuir. 2008; 24:1745–9. [PubMed: 18205422]

74. Pancholi K, Stride E, Edirisinghe M. Dynamics of bubble formation in highly viscous liquids. Langmuir. 2008; 24:4388–93. [PubMed: 18331069]
75. Farook U, Zhang HB, Edirisinghe MJ, et al. Preparation of microbubble suspensions by co-axial electrohydrodynamic atomization. Med Eng Phys. 2007; 29:749–54. [PubMed: 17035065]
76. Feshitan JA, Chen CC, Kwan JJ, et al. Microbubble size isolation by differential centrifugation. J Colloid Interface Sci. 2009; 329:316–24. [PubMed: 18950786]
77. Bohmer MR, Schroeders R, Steenbakkers JAM, et al. Preparation of monodisperse polymer particles and capsules by ink-jet printing. Colloids Surf A Physicochem Eng Aspects. 2006; 289:96–104.
78. Rychak JJ, Lindner JR, Ley K, et al. Deformable gas-filled microbubbles targeted to P-selectin. J Control Release. 2006; 114:288–99. [PubMed: 16887229]
79. Needles A, Couture O, Foster FS. A method for differentiating targeted microbubbles in real time using subharmonic micro-ultrasound and interframe filtering. Ultrasound Med Biol. 2009; 35:1564–73. [PubMed: 19632763]
80. Patil AV, Rychak JJ, Allen JS, et al. Dual frequency method for simultaneous translation and real-time imaging of ultrasound contrast agents within large blood vessels. Ultrasound Med Biol. 2009; 35:2021–30. [PubMed: 19828229]
81. Zheng, H.; Kruse, DE.; Stephens, DN., et al. A sensitive ultrasonic imaging method for targeted contrast microbubble detection. Presented at the 30th Annual International IEEE EMBS Conference; 2008 Aug 20–24; Vancouver, BC.
82. Gessner R, Lukacs M, Lee M, et al. Radiation force-enhanced targeted imaging and near real-time molecular imaging using a dual-frequency high-resolution transducer: in-vitro and in-vivo results. Proc IEEE Ultrason Symp. 2009:9–12.
83. Phillips P. Contrast pulse sequences (CPS): imaging nonlinear microbubbles. Proc IEEE Ultrason Symp. 2001; 2:1739–45.
84. Saracco A, Aspelin P, Leifland K, et al. Bolus compared with continuous infusion of microbubble contrast agent using real-time contrast harmonic imaging ultrasound in breast tumors. Acta Radiol. 2009; 50:854–9. [PubMed: 19634024]
85. Saracco A, Aspelin P, Leifland K, et al. Bolus compared with continuous infusion of microbubble contrast agent using real-time contrast harmonic imaging ultrasound in breast tumors. Acta Radiol. 2009; 50:854–9. [PubMed: 19634024]
86. Needles A, Mehi J, Arditi M, et al. Nonlinear contrast agent imaging with a linear array based micro-ultrasound system. Proc IEEE Ultrason Symp. 2009:279–282.
87. Forsberg F, Rawool NM, Merton DA, et al. Contrast enhanced vascular three-dimensional ultrasound imaging. Ultrasonics. 2002; 40:117–22. [PubMed: 12159917]
88. Dayton PA, Klibanov A, Brandenburger G, et al. Acoustic radiation force in vivo: a mechanism to assist targeting of microbubbles. Ultrasound Med Biol. 1999; 25:1195–201. [PubMed: 10576262]
89. Rychak JJ, Klibanov AL, Ley KF, et al. Enhanced targeting of ultrasound contrast agents using acoustic radiation force. Ultrasound Med Biol. 2007; 33:1132–9. [PubMed: 17445966]
90. Patel D, Dayton P, Gut J, et al. Optical and acoustical interrogation of submicron contrast agents. IEEE Trans Ultrason Ferroelectr Freq Control. 2002; 49:1641–51. [PubMed: 12546146]
91. Patel DN, Bloch SH, Dayton PA, et al. Acoustic signatures of submicron contrast agents. IEEE Trans Ultrason Ferroelectr Freq Control. 2004; 51:293–301. [PubMed: 15128216]
92. Wisner ER, Ferrara KW, Short RE, et al. Sentinel node detection using contrast-enhanced power Doppler ultrasound lymphography. Invest Radiol. 2003; 38:358–65. [PubMed: 12908703]
93. Gao Z, Kennedy AM, Christensen DA, et al. Drug-loaded nano/microbubbles for combining ultrasonography and targeted chemotherapy. Ultrasonics. 2008; 48:260–70. [PubMed: 18096196]

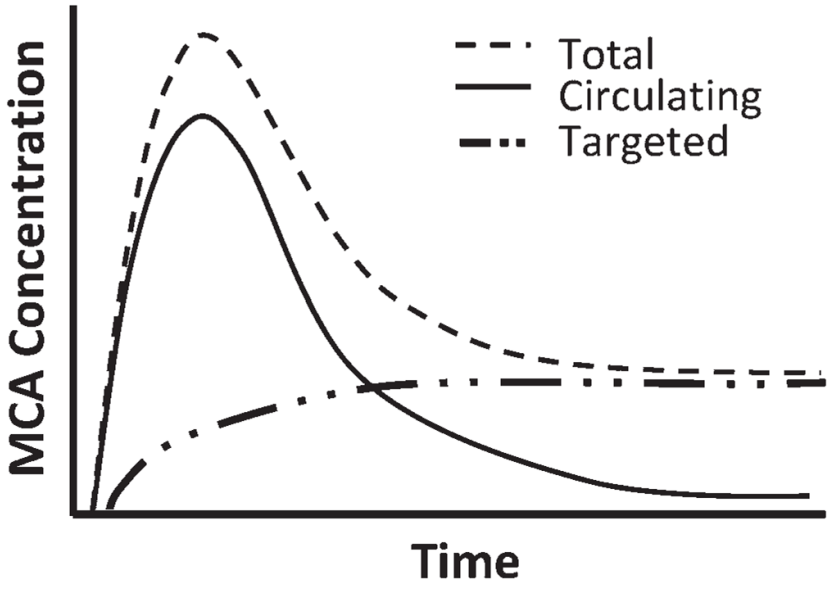

Figure 1.
A cartoon graph illustrating how freely circulating and targeted microbubbles contribute to the overall concentration of contrast within an in vivo environment. Adapted from Christiansen JP and Lindner JR.41 MCA = microbubble contrast agent.

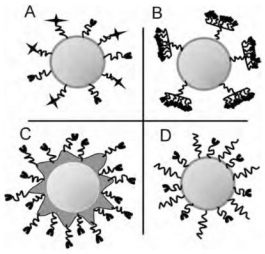

Figure 2.

A schematic showing different microbubble shell and targeting ligand architectures. *A*, Multiple-targeting ligands, such as selectin and immunoglobin adhesion molecules, improve the likelihood of targeting by facilitating a rolling action along vessel walls. *B*, Polymeric forms of targeting ligands promote the likelihood of sustained adhesion. *C*, Excess lipid in shell ("wrinkly bubbles") improves sustained microbubble retention. *D*, Buried-ligand architecture ("stealthy bubbles") reduces both nonspecific binding and immunogenic reactions by veiling targeting ligands from complement proteins until transiently revealed at the desired target site.

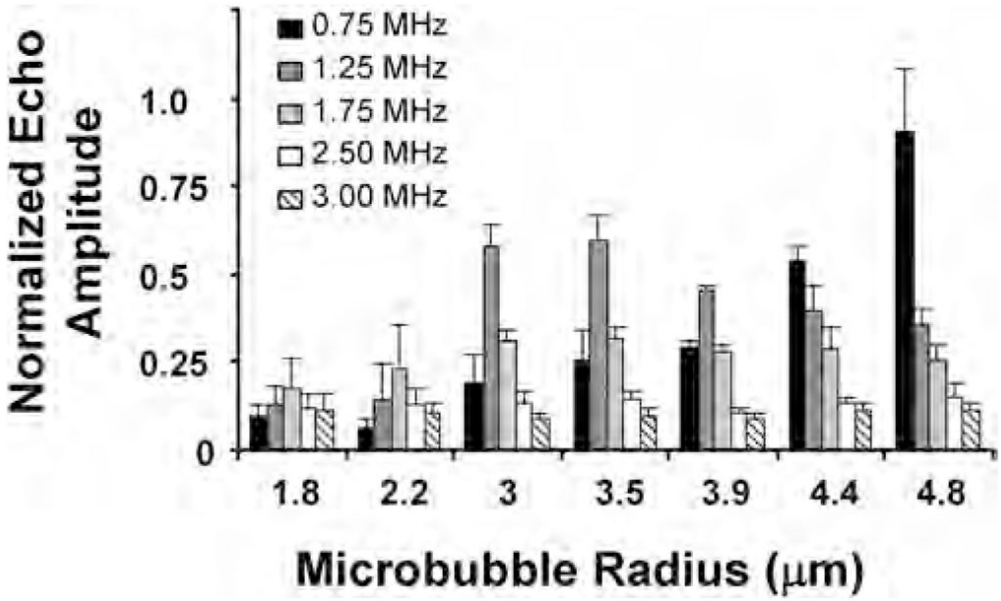

Figure 3.
The relationships between excitation frequency, micro-bubble radius, and resulting echo amplitude. Five-cycle excitation pulses pressure-matched to 100 kPa. Echo amplitudes for each microbubble diameter were maximized near their resonant frequencies, with the greatest achievable response increasing with increasing microbubble size. Adapted from Kaya M et al.47

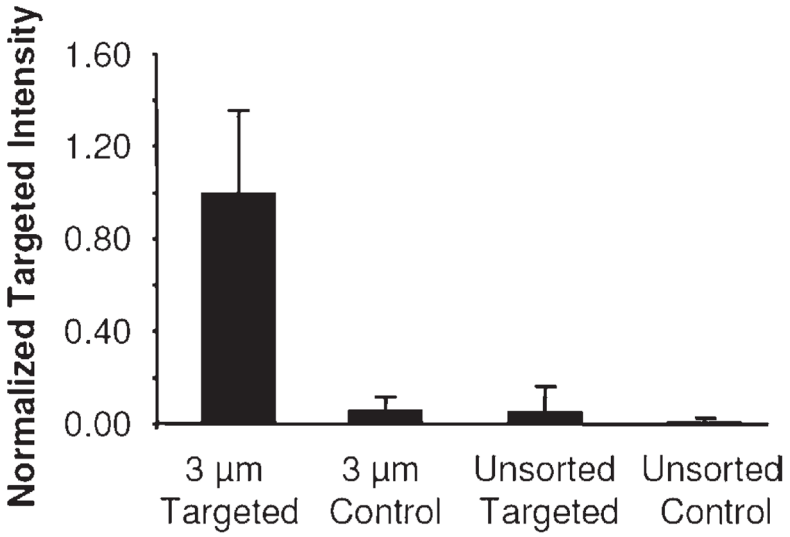

Figure 4.
The relative image intensity improvement between size-isolated large targeted and control microbubbles (*left*) and targeted and control microbubbles with smaller unsorted polydisperse distributions (*right*). Injected concentrations were matched to 3×10^7 bubbles/mL and imaged after freely circulating bubbles had cleared. Reproduced from Streeter JE et al.36

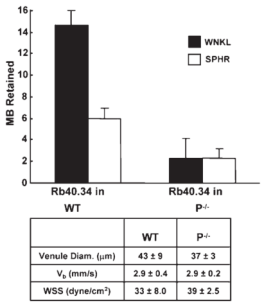

	WT	P-/-
Venule Diam. (μm)	43 ± 9	37 ± 3
V_b (mm/s)	2.9 ± 0.4	2.9 ± 0.2
WSS (dyne/cm²)	33 ± 8.0	39 ± 2.5

Figure 5.

Improvement in targeting retention efficiency of wrinkled (WNKL) microbubbles (MB) compared to traditional spherical (SPHR) microbubbles. Both populations were targeted to P-selectin Rb40.34 with rat monoclonal antibodies. Data acquired using intravital microscopy in 10 different venule locations within both wild-type (WT) and P-selectin-deficient control ($P^{-/-}$) mice, with $n = 4$ and $n = 3$, respectively. Adapted from Rychak JJ et al.78 WSS = wall shear stress.

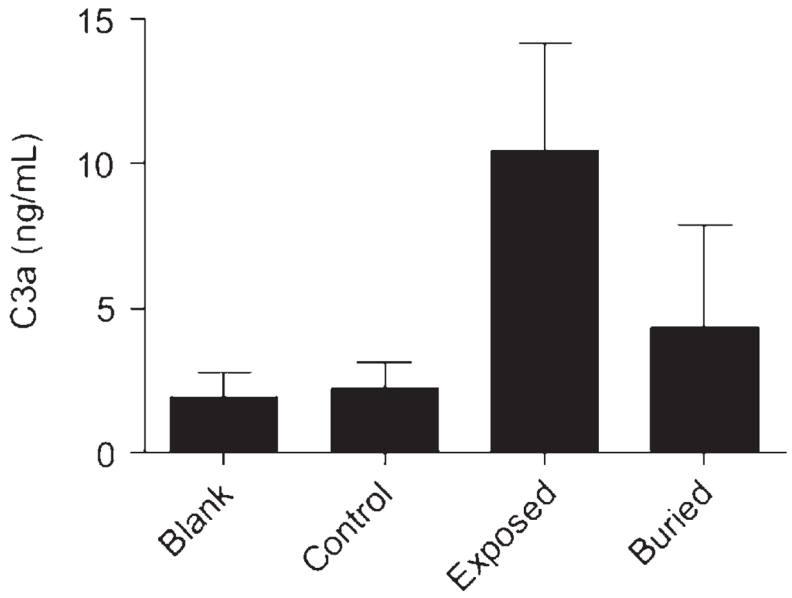

Figure 6.
Enzyme-linked immunosorbent assay analysis illustrating reduced immunogenic response associated with a buried-ligand architecture microbubble compared to a conventional exposed-ligand targeted bubble. Biotin ligands were used in this study. Anaphalatoxin C3a concentration measured after 30-minute in vitro incubation in human serum. “Blank” was PBS only and “control” was a distribution of bubbles bearing no ligand. Adapted from Borden MA et al.56

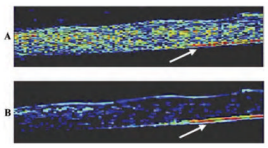

Figure 7.
In vitro images in a flow phantom demonstrating a method to delineate stationary from freely circulating bubbles in real time. Both freely circulating bubbles and stationary bubbles can be seen in A, although in B the signal intensity from freely circulating bubbles is suppressed with a slow-time interframe filter. Bubbles were forced to the distal wall of the vessel with radiation force pulse prior to image collection. The stationary bubble signal is indicated by the *white arrow* in both A and B. Field of view is 4.5 × 18 mm. Adapted from Patil AV et al.80

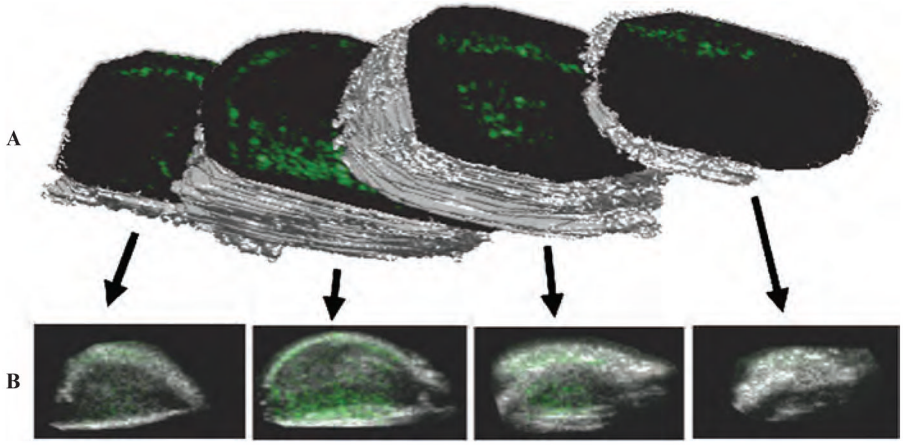

Figure 8.

Three-dimensional molecular imaging of angiogenesis in a rat fibrosarcoma model. The data illustrate the heterogeneity of microbubble targeting throughout the tumor volume (Streeter and colleagues, unpublished data, 2009). *A*, Three-dimensional rendered isosurface produced from B-mode data with manually defined regions of interest around the perimeter. *B*, Corresponding overlaid two-dimensional frames, as seen on an imaging system, prior to three-dimensional reconstruction. Grayscale anatomic images were collected with B-mode, whereas green overlaid contrast-only images were collected with Siemens contrast pulse sequence (Mountain View, CA).

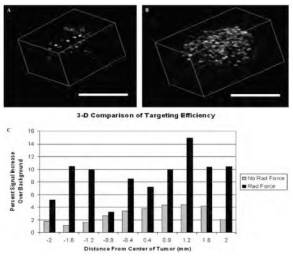

Figure 9.

Images and data illustrating the improvement in targeting efficiency facilitated by the application of radiation force (RF) in an angiogenic rat tumor model. A and B are three-dimensional reconstructions of two-dimensional imaging planes acquired after freely flowing bubbles cleared from the system. *A*, RF not administered. *B*, RF pulses administered for 15 seconds after bolus injection of contrast. Scale bars are 1 cm. *C*, Plot comparing targeted signal between acquisitions with RF application and without. A mean signal increase of 13 dB was observed across all slices in response to RF. Adapted from Gessner R et al.82